Prebiotic Synthesis of Sugar and Molecular Dynamic Simulation of 2,3-Dihydroxypropanal Adsorption on Montmorillonite

Vojood, Arash; Khodadadi Moghaddam, Mohammad*+;
Ebrahimzadeh Rajaei, Gholamreza*+; Mohajeri, Sahar; Shamel, Ali
Department of Chemistry, Ardabil Branch, Islamic Azad University, Ardabil, I.R. IRAN

ABSTRACT: *This study initially investigated sugar production through a Formose Reaction (FR) using methanol as a solvent and an aerosil (fumed silica) as a catalyst. The products observed in the reaction medium were 2,3-dihydroxypropanal (glyceraldehyde) and 1,2-ethanediol (ethylene glycol). The results showed that if the target of the reaction is to produce glyceraldehyde (GA) and ethylene glycol (EG), the aerosil is a better option as a catalyst in the FR. Finally, the Molecular Dynamic (MD) simulation of 2,3-dihydroxypropanal adsorption was investigated on montmorillonite (MMT) as a mineral adsorbent. MD simulation indicated that the adsorption of GA molecule at the MMT-water interface occurred due to the oxygen of the carbonyl group. The Radial Distribution Function (RDF) of the solvent around the main atoms of GA and the Root-Mean-Square Deviation (RMSD) were calculated from the MD simulation results using Gaussian and LAMMPS software. The RDF results showed a weak hydrogen bond between oxygen atoms of the hydroxyl group and solvent molecules. Moreover, the solvent molecules had no significant influence on the behavior of tetrahedral carbons of GA, indicating that the oxygen atom of the carbonyl group had a higher ability to form a hydrogen bond with water compared to the other atoms. The RMSD of carbonyl oxygen, carbonyl carbon, hydroxyl oxygen, and tetrahedral carbon increased during a simulation time of 20 ns, respectively. Evaluation of the mean distance of calcium atom at the surface of MMT and different atoms of GA showed that the GA molecule was chemically adsorbed on the surface of MMT by oxygen of carbonyl. The mean distances of C-tetrahedral, C-carbonyl, O-hydroxyl, and O-carbonyl in the GA structure from the surface of MMT (distance from calcium ions) were estimated to be 3.8, 3.2, 3.0, and 2.6 Å, respectively.*

KEYWORDS: *Origin of life; Formose reaction; Glyceraldehyde; Montmorillonite; Adsorption; Molecular dynamic.*

INTRODUCTION

Studies have shown that biomolecules such as amino acids, heterocyclic molecules, and sugars (materials related to the origin of life) must have existed for the formation of polysaccharides before the advent of life on the planet [1-3]. Monosaccharides, or sugars, along with the fats and proteins are among the important building

blocks of life. In addition, they created the basis of living matter with the approximate mass of 2.5×10^{18} g of the carbon on the Earth [4-5].

The compound 2,3-dihydroxypropanal is a colorless solid, and sweet triose monosaccharide with one asymmetric or chiral carbon and two hydroxyl groups on the positions of 2 and 3. This optically active compound can be found in two spatial isomeric forms; R (clockwise) and D (counterclockwise) [3, 6-10]. On the other hand, studies on the FR, which was first discovered in 1861 by a Russian chemist named Alexander Mikhaylovich Butlerow, indicated that the prebiotic synthesis of sugars is performed through this reaction. In this regard, GA biomolecules can be synthesized under prebiotic conditions through non-biological reactions of carbohydrate production [11-16]. This compound can be naturally found in the body of living creatures including the human [9]. *Lambert et al.* [17] studied the role of silicates in the synthesis of sugars under prebiotic conditions and presented the FR mechanism for the production of GA monosaccharides.

Nowadays, alongside experimental approaches, computer-based simulations have considerably contributed to the understanding of physical phenomena and can provide a direct way to describe the microscopic features of a system, including its interactions and molecular structure. Among these novel techniques, Molecular Dynamics (MD) simulations have received the attention of researchers as a statistical mechanics-based method [18-25]. This method was first introduced by Alder and Wainwright in the late 1950s [26, 27]. This method will undoubtedly be used in the future to explore carbohydrates [28].

Feng et al. [20] examined food carbohydrates by MD simulations and provided a general idea of how to use this method in the studies of edible carbohydrates. The results of this study showed that MD simulations offer several advantages despite their disadvantages. In another study, Fadda and Woods [29] examined carbohydrates and their associated issues through modeling. *Madsen et al.* [28] also addressed sugars and their solvation through MD simulation and introduced the basic techniques used in their simulation. *Frank et al.* [30] also used MD simulations for conformational analysis of oligosaccharides (a saccharide polymer containing a small number of monosaccharides). In this study, the use of MD simulation data to analyze the conformational features of oligosaccharides has been described.

Based on geological studies, bentonite was formed as a result of alteration of molten magma and volcanic ash in the depth of the seas or upon exposure to various climate conditions. Bentonite was first discovered in the Montmorillon Mine in France in 1847, and was named MMT [31, 32]. As a member of clay family and belonging to a series of minerals from the smectites group, MMT has a layered structure and can act as a suitable and versatile catalyst for various types of organic reactions. Due to its unique physical and chemical properties, this clay mineral has found wide industrial and research applications [33-39].

Liu et al. [40] and Greathouse and Cygan [41] respectively applied MD simulation for studying the adsorption of benzene and uranyl (VI) on the surface of MMT. Khodadadi-Moghaddam and Sarabi-Aghbolagh [42] investigated the interaction of oligomer chains of tri-bisphenol-A-diglycidyl ether with calcium-containing MMT using MD simulations. Their research showed that the adsorption of oligomer chains on the surface of MMT is carried out through the etheric oxygen atoms of the chain. Therefore, in the present study, MD modeling was used to explore the adsorption of simple GA sugar, synthesized by FR in the presence of a heterogeneous catalyst under certain conditions such as temperature and pH, on the calcium-containing MMT.

EXPERIMENTAL SECTION
Materials and equipment

Acetone (pure grade), hydrochloric acid 37% (analytical purity grade), methanol (GC grade), and sodium sulfate (dehydrated) were purchased from Merck, and aerosil (fumed silica) from Sigma-Aldrich. Moreover, aqueous solution of formaldehyde 37% (pure grade) and sodium hydroxide (guaranteed grade), which was used as a strong base, were purchased from Shimi Delta Company.

Sugar analysis of the samples was performed using the Agilent 5975C GCMS equipment. Effective and mild separation of liquid phases of the samples was conducted through evaporation by an RE200 rotary evaporator from Bibby. Moreover, a WTW inoLab 720 pH meter was used to adjust the pH of the solutions. An HO502 Heater Stirrer from Bibby was used to control the temperature. An electronic analytical balance (Scaltel, SPB55-Germany, with an ability to read up to an accuracy of 0.0001 g) was used for weighing the solid materials. A centrifuge model 155 from Zag Chemie Company was used to separate

the solid particles of the samples before injecting them into a GC-MS device.

Formose procedure for the synthesis of sugar

In this work, 100 mL of methanol with 11 mL of aqueous formaldehyde solution (formalin) was first transferred to a 250-mL three-necked flask and heated up to a temperature of 60 ℃. Then, 2 M sodium hydroxide solution was added to bring it to the desired pH (7.8), and finally, 0.08 g of the aerosil catalyst was added to the flask to start the reaction. Furthermore, from the beginning of the reaction until the end, a condenser was attached to a three-necked flask the end of which was blocked by some cotton, sodium sulfate (dehydrated), and a thick balloon. Nitrogen gas continuously flowed into the flask, and the temperature was constantly monitored to remain between 55 and 65 ℃. Then, at the desired intervals, 5 mL of the mixture was taken and immediately acidified with a solution of 6 N hydrochloric acid (HCl) to stop the reaction. A small amount of water was entered into the system along with a hydrochloric acid solution, and no more water was added to the system. The liquid samples were then dried in a rotary evaporator until they turned into white solid samples, and after dissolving these solid samples in 5 mL of methanol, they were centrifuged for analysis in a GC-MS device [43, 44].

COMPUTATIONAL DETAILS

In this work, one GA molecule ($C_3H_6O_3$) was simulated on a layer of calcium-containing MMT ($Al_2Ca_{0.5}O_{12}Si_4$), (amcsd database code: AMCSD#0002867) [37, 45] in a $2\times5\times5$ unit cell (x,y,z). The GA molecule was first plotted in GaussView 06 software and then optimized by Gaussian 09 software using MD methods. The optimized molecule was then placed at a proper distance from the MMT surface and its behavior was addressed in the water-MMT interface throughout the simulation duration.

The simulation box was an orthorhombic cell with a dimension of $25.8\times43.2\times120.0$ Å along x, y, and z directions, respectively. A total of 9026 atoms exists in this simulation box. The atoms were assumed to be rigid and their charge polarization was neglected. Periodic boundary conditions were considered in all directions.

MD simulations were carried out in LAMMPS software. Temperature stabilization at 298 K was achieved through the integration of the velocity equations in an NVT ensemble in which the number of particles, volume, and temperature were considered constant. The integration time interval was set at 100 ps. For pressure stabilization at 1 atm, integration of the velocity equations was carried out on an NPT ensemble in which the number of particles, pressure, and temperature were considered constant. The time interval to solve the dynamic equations was 1 ns. For sampling and data extraction, the dynamic equations were solved for a 20-ns interval.

The Nose-Hoover algorithm was employed to keep the temperature and pressure constant. The standard deviation of the temperature and pressure was 5.08 K and 0.13 atm in the data sampling stage, respectively. The equations of motion were integrated by the Verlet algorithm in 1-femtosecond steps. In addition, the cut-off distance was 12 Å. The COMPASS force field [46, 47] was successfully utilized to simulate the polymeric structure, while the CLAYFF force field was used to model MMT [48].

RESULTS and DISCUSSION

Formose reaction in methanol solvent

Figs. 2 and 3 show the results of the FR at pH =7.8 in the presence of a heterogeneous aerosil catalyst. GA monosaccharide and EG are the two main products of the FR under the conditions applied during this project [44, 49].

Fig. 1 shows the synthesis of GA in the methanol solvent. According to the figure, the amount of GA slowly increases during the process and reaches a maximum of 0.04 mmol/dL, and at this concentration, a steady state is formed. The reason for this behavior is to balance the rate of production of EG and its rate of conversion to GA.

Fig. 2 shows the amount of EG produced in the methanol solvent over time. The amount of EG in the mixture increases from the beginning of the reaction and reaches a maximum amount of 0.89 mmol/dL during 540-630 minutes. Moreover, the amount of this substance reaches a stable state at a concentration of 0.89 mmol/dL. Due to the FR mechanism and the fact that high-carbon sugars are made from low-carbon sugars, the reason for reaching a steady state after long periods of time can be attributed to the balance in the rate of EG sugar synthesis and its conversion rate to the GA biomolecule.

Radial Distribution Function (RDF)

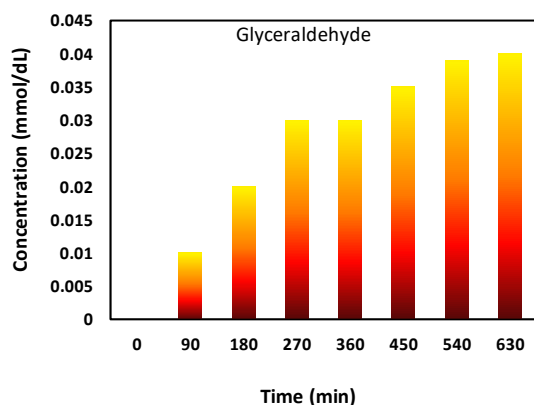The radial distribution function of the solvent around the atoms can be a good criterion for atomic interactions

Fig. 1: Changes in GA concentration produced in the methanol solvent over time through FR at pH =7.8.
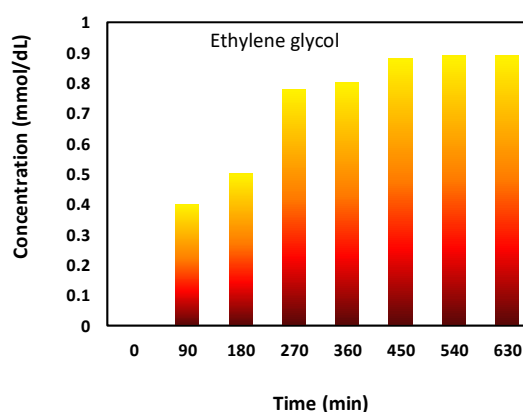

Fig. 2: Changes in EG concentration produced in the methanol solvent over time through FR at pH = 7.8.

with the surrounding and their general behavior. Fig. 3 represents the RDF of water around the various atoms of GA. In case of tetrahedral carbon, there is no proper order in the molecules around the carbons. Moreover, the main peak of the water molecules can be seen at a relatively long distance (about 5 Å). Lack of proper regularity and the long distance of water molecules from tetrahedral carbon indicate a weak interaction between them. It can be concluded that the tetrahedral carbon of the GA is in weak interaction with the water molecules and is surrounded by them at long distances [50]. Therefore, the solvent molecules will have no significant influence on the behavior of tetrahedral carbons of GA molecules.

Fig. 3 indicates stronger interaction of water molecules with carbonyl carbons. The first layer of water around the carbonyl carbon was observed at a distance of 2.5 Å and the main layer (the second one) emerged at a distance of 3 Å. The regularity of this type of water molecule around the carbon atoms and the observed peak intensity indicates the formation of hydrogen bonds between water molecules and carbonyl carbon atoms in the GA. Therefore, it can be concluded that the solvent plays a decisive role in the behavior and reactivity of the carbonyl carbon of GA.

A comparison of the RDF of carbonyl carbon and carbonyl oxygen in Fig. 3 shows that the oxygen atom of the carbonyl group has a higher ability to form a hydrogen bond with water as compared with carbonyl carbons. The shorter distance of water molecules from the oxygen of the carbonyl group and their better arrangement suggest a stronger interaction between oxygen atoms of the carbonyl group and the solvent molecules. Therefore, it can be concluded that the behavior of the oxygen atom of

the carbonyl group in the GA molecule is strongly influenced by the solvent.

Finally, the solvation of oxygen atoms of the hydroxyl group with water was represented in Fig. 3. A comparison of the RDFs of carbonyl and hydroxyl oxygens indicates the weakness of hydroxyl oxygen in establishing hydrogen bonds and order in the surrounding water molecules compared to the carbonyl oxygen. A comparison of these two figures revealed that both the number of water molecules around hydroxyl oxygen and their regularity were less than the oxygen atom of the carbonyl group. However, a weak hydrogen bond was established between oxygen atoms of the hydroxyl group and solvent molecules.

Root-Mean-Square Deviation (RMSD)

RMSD indicates the mobility of atoms during simulation. Fig. 4 shows the RMSD of tetrahedral and carbonyl carbons as well as carbonyl and hydroxyl oxygen atoms in the GA molecule. According to Fig. 4, the lowest RMSD was observed for the oxygen of carbonyl. Due to its stronger interactions with the solvent, this atom exhibited less mobility. Subsequently, RMSD of carbonyl carbon, hydroxyl oxygen, and tetrahedral carbon increased, respectively.

On the other hand, investigation results on RMSD were consistent with the RDF results. Carbonyl oxygen, which showed the highest interaction with the solvent, exhibited the least mobility, while tetrahedral carbon was the most mobile atom with the least interaction.

Mean distance from the surface

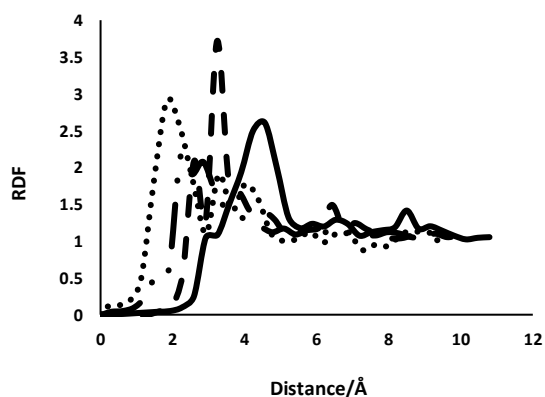Fig. 5 shows the mean distance of different atoms of GA from the MMT surface (distance from the calcium ions)

Fig. 3: RDF of water molecules around tetrahedral carbon (solid line), carbonyl carbon (- - -), carbonyl oxygen (……), and hydroxyl oxygen (-..-..) in GA molecule adsorption on the surface of MMT.
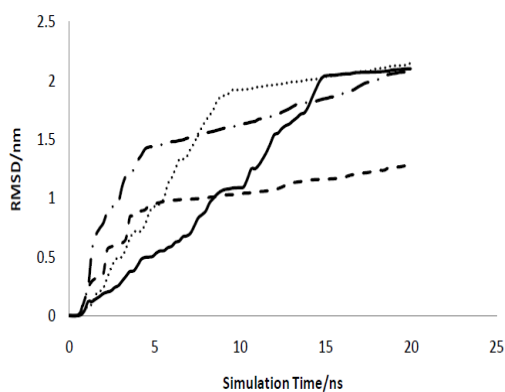

Fig. 4: RMSD of tetrahedral carbon (solid line), carbonyl carbon (_._._), carbonyl oxygen (------), and hydroxyl oxygen (……) in the GA molecule adsorption.
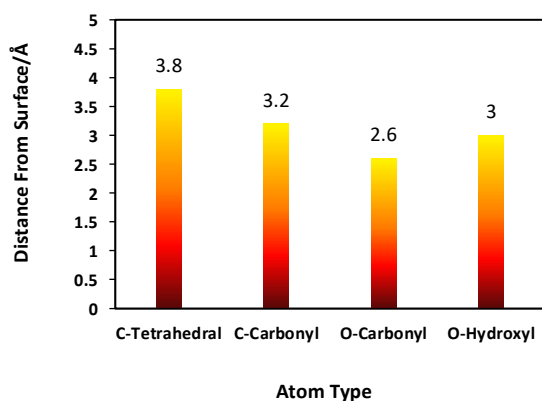

Fig. 5: Mean distance of GA atoms from the surface of MMT (distance from calcium ions) during the simulation.

during the simulation. An investigation of this diagram indicates that tetrahedral carbon has the farthest distance from the surface of MMT. This distance was about 3.8 Å, indicating a weak physical interaction between this atom and the MMT surface. Regarding Fig. 4, such a weak interaction leads to greater mobility of tetrahedral carbons than others.

The distance between the carbonyl carbon and hydroxyl oxygen from the surface of MMT was lower than tetrahedral carbon (3.2 and 3.0 Å, respectively). This distance indicates a stronger interaction with the surface, which also justifies the lower mobility of these atoms. However, it should be noted that this distance is still too large for the interaction between these two atoms and the surface of MMT to be chemical.

Finally, the mean distance of a carbonyl oxygen atom from the surface of MMT (distance from calcium ions) was about 2.6 Å, which is in the range of chemical adsorption. These results indicate that the GA biomolecule is chemically adsorbed on the surface of MMT by carbonyl oxygen. Thus, this explains the considerably lower mobility of this atom compared to other atoms (see Fig. 5).

CONCLUSIONS

In this study, the FR (non-biological reaction to produce sugars) was first performed in the presence of a mineral-fumed silica catalyst. The products observed in this reaction include GA and EG. The present study shows that if the target of the reaction is to produce GA and EG, an aerosol is a useful option catalyst in the FR. Finally, the adsorption of GA biomolecule at the MMT-water interface was investigated by MD simulation. The simulation findings indicated that the GA molecule was adsorbed on the surface of MMT (distance from calcium ions) through the oxygen of carbonyl, while the other atoms were relatively far from the surface and physically interacted with the adsorbent surface.

The RMSD values during the simulation showed that the carbonyl oxygen atoms had the least mobility while the tetrahedral carbon atoms were the most mobile ones. The mobility of hydroxyl oxygen and carbonyl carbon atoms was almost at the same level. This finding is well correlated with the distance of atoms from the surface of MMT. It can be concluded that the carbonyl oxygen atom was chemically adsorbed due to its proximity to the surface and as a result, showed less mobility during the simulation.

Other atoms showed higher mobility than carbonyl oxygen by increasing the distance from the surface.

Investigation of the radial distribution function of water molecules around GA biomolecule indicated that carbonyl oxygen and tetrahedral carbon had the highest and lowest interactions with water, respectively. The interaction of hydroxyl oxygen and carbonyl carbon atoms was almost similar. MD simulation data suggested the chemical adsorption of GA on the surface of MMT through carbonyl oxygen. Moreover, the greater solvation of the carbonyl oxygen atom than the other atoms indicates a stronger hydrogen bond for this part of the molecule with the solvent.

Acknowledgments

REFERENCES

[1] Lambert J.B., Guruswamy-Thangavelu S.A., In: Zelisko P.M., (ed) "Bio-Inspired Silicon-Based Materials". Springer, Berlin, Heidelberg (2014).

[2] Ichihashi N., Yomo T., Constructive Approaches for Understanding the Origin of Self-Replication and Evolution, *Life*., **6(3)**: 26 (2016).

[3] Pascal R., Boiteau L., Auguste Commeyras A., In: Walde P., (ed) "Prebiotic Chemistry from Simple Amphiphiles to Protocell Models". Springer, Berlin, Heidelberg (2005).

[4] Zhou X., Dalai P., Sahai N., Semipermeable Mixed Phospholipid-Fatty Acid Membranes Exhibit K^+/Na^+ Selectivity in the Absence of Proteins, *Life.*, **10(4)**: 39 (2020).

[5] Niaza K., Khanb F., Ajmal Shah M., In: Sanches Silva A., Seyed Nabavi F., Saeedi M., Seyed Nabavi M., (eds) "Recent Advances in Natural Products Analysis". 5th ed., Elsevier, Amsterdam (2020).

[6] Pestunova O., Simonov A., Snytnikov V., Stoyanovsky V., Parmon V., Putative Mechanism of the Sugar Formation on Prebiotic Earth Initiated by UV-Radiation, *Adv. Space Res.,* **36(2)**: 214-219 (2005).

[7] Lamour S., Pallmann S., Haas M., Trapp O., Prebiotic Sugar Formation Under Nonaqueous Conditions and Mechanochemical Acceleration, *Life.,* **9(2)**: 52 (2019).

[8] Moldoveanu S.C., Pyrolysis of Carbohydrates, *Tech. Instrum. Anal. Chem.,* **28**: 419-470 (2010).

[9] Clough S.R., In: Wexler P., (ed) "Encyclopedia of Toxicology". 3rd ed., Elsevier, Amsterdam (2014).

[10] Stovbun S.V., Zanin A.M., Shashkov M.V., Skoblin A.A., Zlenko D.V., Tverdislov V.A., Mikhaleva M.G., Taran O.P., Parmon V.N., Spontaneous Resolution and Super-coiling in Xerogels of the Products of Photo-Induced Formose Reaction, *Orig Life Evol. Biosph*., **49(3)**: 187-196 (2019).

[11] Omran A., Menor-Salvan C., Springsteen G., Pasek M., The Messy Alkaline Formose Reaction and Its Link to Metabolism, *Life.,* **10(8)**: 125 (2020).

[12] Weber A.L., Prebiotic Sugar Synthesis: Hexose and Hydroxy Acid Synthesis from Glyceraldehyde Catalyzed by Iron (III) Hydroxide Oxide, *J. Mol. Evol.,* **35(1)**: 1–6 (1992).

[13] Butlerow A., Bildung einer zuckerartigen Substanz Durch Synthese, *Justus Liebigs Ann. Chem.,* **120(3)**: 295-298 (1861).

[14] Michitaka T., Imai T., Hashidzume A., Formose Reaction Controlled by a Copolymer of N,N-Dimethylacrylamide and 4-Vinylphenylboronic Acid, *Polymers.,* **9(11)**: 549 (2017).

[15] Shapiro R., Prebiotic Ribose Synthesis: A Critical Analysis, *Origins Life Evol. Biospheres.,* **18(1-2)**: 71-85 (1988).

[16] Toxaverd S., Homochirality in Bio-Organic Systems and Glyceraldehyde in the Formose Reaction, *J. Biol. Phys.,* **31(3-4)**: 599-606 (2005).

[17] Lambert J.B., Guruswamy-Thangavelu S.A., Ma K., The Silicat-Mediated Formose Reaction: Bottom-Up Synthesis of Sugar Silicat, *Science.,* **327(5968):** 984-986 (2010).

[18] Veszprémi T., Fehér M., In: Veszprémi T., Fehér M., (eds) *"Quantum Chemistry"*. Springer, Boston (1999).

[19] Nabati M., Bodaghi-Namileh V., Molecular Modeling of 3-(1,3-Dioxoisoindolin-2-yl) Benzyl Nitrate and Its Molecular Docking Study with Phosphodiesterase-5 (PDE5), *Adv. J. Chem. A.,* **3(1):** 58-69 (2020).

[20] Feng T., Li M., Zhou J., Zhuang H., Chen F., Ye R., Campanella O., Fang Z., Application of Molecular Dynamics Simulation in Food Carbohydrate Research-A Review, *Innovative Food Sci. Emerging Technol.,* **31**: 1-13 (2015).

Research Article

[21] Rapaport D.C., *"The Art of Molecular Dynamics Simulation"*, 2nd ed., Cambridge University Press, Cambridge (2004).

[22] Rezazadeh Mofradnia S., Ashouri R., Abtahi N., Yazdian F., Rashedi H., Sheikhpour M., Ashrafi F., Production and Solubility of Ectoine: Biochemical and Molecular Dynamics Simulation Studies, *Iran. J. Chem. Chem. Eng. (IJCCE),* **39(6)**: 259-269 (2020).

[23] Board Jr J.A., Causey J.W., Leathrum Jr J.F., Windemuth A., Schulten K., Accelerated Molecular Dynamics Simulation with the Parallel Fast Multipole Algorithm, *Chem. Phys. Lett.,* **198(1-2)**: 89-94 (1992).

[24] Haile J.M., "Molecular Dynamics Simulation: Elementary Methods", 1st ed., Wiley, New York (1992).

[25] Yusuff O.K., Tunde Raji A., Abdul Raheem M.A.O., Boluwaji Ojo D., Explicit Solvent Molecular Dynamics Simulation Studies of the Dissociation of Human Insulin Hexamer into the Dimeric Units, *Adv. J. Chem. A.,* **3**: 730-739 (2020).

[26] Alder B.J., Wainwright T.E., Phase Transition for a Hard Sphere System, *J. Chem. Phys.,* **27(5)**: 1208-1209 (1957).

[27] Alder B.J., Wainwright T.E., Studies in Molecular Dynamics. I. General Method, *J. Chem. Phys.,* **31(2)**: 459-466 (1959).

[28] Madsen L.J., Ha S.N., Tran V.H., Brady J.W., In: French A.D., Brady J.W., (eds) "Computer Modeling of Carbohydrate Molecules", American Chemical Society, Washington D.C (1990).

[29] Fadda E., Woods R.J., Molecular Simulations of Carbohydrates and Protein–Carbohydrate Interactions: Motivation, Issues and Prospects, *Drug Discovery Today.*, **15(15-16)**: 596-609 (2010).

[30] Frank M., In: Lütteke T., Frank M., (eds) "Glycoinformatics". Humana Press, New York (2015).

[31] Cseri T., Békássya S., Bódás Z., Ágai B., Figueras F., Acetylation of B15C5 Crown Ether on Cu Modified Clay Catalysts, *Tetrahedron Lett*., **37(9)**: 1473-1476 (1996).

[32] Almasri D.A., Rhadfi T., Atieh M.A., McKay G., Ahzi S., High Performance Hydroxyiron Modified Montmorillonite Nanoclay Adsorbent for Arsenite Removal, *Chem. Eng. J.,* **335**: 1-12 (2018).

[33] Tyagi B., Chudasama C.D., Jasra R.V., Determination of Structural Modification in Acid Activated Montmorillonite Clay by FT-IR Spectroscopy, *Spectrochim. Acta, Part A.,* **64(2)**: 273-278 (2006).

[34] Darvish M., Moradi Dehaghi S., Taghavi L., Karbassi A.R., Removal of Nitrate Using Synthetic Nano Composite ZnO/Organoclay: Kinetic and Isotherm Studies, *Iran. J. Chem. Chem. Eng. (IJCCE),* **39(1)**: 105-118 (2020).

[35] Bhattacharyya K.G., Guptab S.S., Adsorption of a Few Heavy Metals on Natural and Modified Kaolinite and Montmorillonite: A Review, *Adv. Colloid Interface Sci*., **140(2)**: 114-131 (2008).

[36] Zhang D., Zhou C.H., Lin C.X., Tong D.S., Yu W.H., Synthesis of Clay Minerals, *Appl. Clay Sci.,* **50(2)**: 1-11 (2010).

[37] Uddin F., In: Zoveidavianpoor M., (ed) "Current Topics in the Utilization of Clay in Industrial and Medical Applications". IntechOpen, London (2018).

[38] Shamsipur M., Bahrami Adeh N., Sadegh Hajitarverdi M., Zarei F., Yazdimamaghani M., Synthesis and Properties of Plasticized Sulfur-Montmorillonite Nanocomposites by Melt-Blending, *Iran. J. Chem. Chem. Eng. (IJCCE),* **36(6)**: 1-9 (2017).

[39] Terán E.J., Montes M.L., Rodríguez C., Martino L., Quiroga M., Landa R., Torres Sánchez R.M., Díaz Pace D.M., Assessment of Sorption Capability of Montmorillonite Clay for Lead Removal from Water Using Laser–Induced Breakdown Spectroscopy and Atomic Absorption Spectroscopy, *Microchem J.,* **144**: 159-165 (2019).

[40] Liu X., Zhu R., Ma J., Ge F., Xu Y., Liu Y., Molecular Dynamics Simulation Study of Benzene Adsorption to Montmorillonite: Influence of the Hydration Status, *Colloids Surf., A,* **434**: 200-206 (2013).

[41] Greathouse J.A., Cygan R.T., Molecular Dynamics Simulation of Uranyl (VI) Adsorption Equilibria onto an External Montmorillonite Surface, *Phys. Chem. Chem. Phys.,* **7(20):** 3580-3586 (2005).

[42] Khodadadi-Moghaddam M., Sarabi-Aghbolagh S., Molecular Dynamic Simulation of Adsorption of tri-Bisphenol-A-Diglycidyl Ether on Montmorillonite, Nashrieh Shimi va Mohandesi Shimi Iran (NSMSI), **38(2)**: 173-182 (2019), [in Persian.

[43] Vojood A., Khodadadi Moghaddam M., Ebrahimzadeh-Rajaei G., Mohajeri S., Shamel A., Increasing in the Selectivity of Formose Reaction for Glyceraldehyde Production in the Presence of Fumed Silica and Montmorillonite Catalysts, *Chem. Methodol.* **5(5)**: 422-432 (2021).

[44] Vojood A., Khodadadi Moghaddam M., Ebrahimzadeh-Rajaei G., Mohajeri S., Shamel A., Comparison of Selectivity of Ethylene Glycol Synthesis and Glyceraldehyde Biomolecule through Formose Reaction in Water and Methanol Solvent, *J. of Applied Chemistry.*, **17(63)**: 39-51 (2022), [in Persian].

[45] Viani A., Gualtieri A.F., Artioli G., The Nature of Disorder in Montmorillonite by Simulation of X-ray Powder Patterns, *Am. Minral.*, **87(7)**: 966-975 (2002).

[46] Scocchi G., Posocco P., Fermeglia M., Pricl S., Polymer-Clay Nanocomposites: A Multiscale Molecular Modeling Approach, *J. Phys. Chem. B.*, **111(9)**: 2143-2151 (2007).

[47] Abdulfatai U., Uzairu A., Uba S., Shallangwa G., Quantitative Structure-Properties Relationship of Lubricating Oil Additives and Molecular Dynamic Simulations Studies of Diamond-Like-Carbon (DLC), *Iran. J. Chem. Chem. Eng. (IJCCE)*, **39(4)**: 281-295 (2020).

[48] Cygan T.R., Liang J.J., Kalinichev A.G., Molecular Models of Hydroxide, Oxyhydroxide, and Clay Phases and the Development of a General Force Field, *J. Phys. Chem. B.*, **108(4)**: 1255-1266 (2004).

[49] Yue H., Zhao Y., Maa X., Gong J., Ethylene Glycol: Properties, Synthesis, and Applications, *Chem Soc Rev.*, **41(11)**: 4089-4380 (2012).

[50] Ebrahimzadeh Rajaei G., Vojood A., Investigation of the Specific Ion Interactions and Determining Protonation Constant of 3,5-Dihydroxy-2-(3,4,5-trihydroxybenzoyl)oxy-6-[(3,4,5-trihydroxybenzoyl)oxymethyl] oxan-4-yl] 3,4,5-trihydroxybenzoate at Different Ionic Strength, *Iran. J. Chem. Chem. Eng. (IJCCE)*, **38(5)**: 91-98 (2019).